Journal of Engineering Science and Technology
Vol. XX, No. Y (Year) PPP - QQQ

FAULT DIAGNOSIS IN ROTATING MACHINE USING FULL SPECTRUM OF VIBRATION AND FUZZY LOGIC

ROGER R. DA SILVA, EDNELSON DA S. COSTA,
ROBERTO C. L. DE OLIVEIRA, ALEXANDRE L. A. MESQUITA*

Federal University of Pará, Institute of Technology, Augusto Correa St 1, P.O. Box 479, 66075-110, Belém-PA, Brazil
*Corresponding Author: alexmesq@ufpa.br

Abstract

Industries are always looking for more efficient maintenance systems to minimize machine downtime and productivity liabilities. Among several approaches, artificial intelligence techniques have been increasingly applied to machine diagnosis. Current paper forwards the development of a system for the diagnosis of mechanical faults in the rotating structures of machines, based on fuzzy logic, using rules foregrounded on the full spectrum of the machine´s complex vibration signal. The diagnostic system was developed in Matlab and it was applied to a rotor test rig where different faults were introduced. Results showed that the diagnostic system based on full spectra and fuzzy logic is capable of identifying with precision different types of faults, which have similar half spectrum. The methodology has a great potential to be implemented in predictive maintenance programs in industries and may be expanded to include the identification of other types of faults not covered in the case study under analysis.

Keywords: Vibration, Rotor, Full Spectrum, Fuzzy Logic, Fault Diagnosis.

1. Introduction

Faults in machinery may generate economic loss and safety problems due to unexpected and sudden production stoppages. An efficient maintenance may detect faults at an early stage and minimize shutdown of the machine and costs, with increased safety, reliability and productivity. However, a good maintenance plan requires robust data acquisition, signal processing system and effective fault diagnosis methodology [1]. Nowadays, there is a trend towards condition-based maintenance or prediction maintenance program by employing advanced signal processing techniques and using them as an input to artificial intelligence (AI) approach for diagnostics.

Nomenclature

$A1X_+$	Amplitude of the first positive harmonic, m^2/s^2Hz
$A1X_-$	Amplitude of the first negative harmonic, m^2/s^2Hz
$p(t)$	Complex coordinate
S_{yy}	Auto spectral density function of $y(t)$, m^2/s^2Hz
S_{yz}	Cross-spectral density function between $y(t)$ and $z(t)$, m^2/s^2Hz
S_{zy}	Cross-spectral density function between z(t) and y(t), m^2/s^2Hz
S_{zz}	Auto spectral density function of $z(t)$, m^2/s^2Hz
S_{pp}	Directional power spectral density function, m^2/s^2Hz
X	Rotation of the machine, Hz
$y(t)$	Real coordinate
$Y3_+$	Percentage ratio of amplitudes in positive frequency spectrum
$Y3_-$	Percentage ratio of amplitudes in negative frequency spectrum
$z(t)$	Real coordinate

Greek Symbols

ω	Rotational speed, rad/s

Abbreviations

ARMA	Autoregressive moving average
dPSD	Directional power spectral density function
dCSD	Directional cross-spectral density function
FFT	Fast Fourier transform
RMS	Root Mean Square

Signal processing techniques for fault diagnosis have been the object of intense research and have generated several methodologies during the last 30 years [2]. Specialized literature mentions three categories of signal processing techniques for vibration analysis: time-domain, frequency domain and time-frequency domain analyses [1]. Time-domain analyses comprise, for example, mean value, peak, peak-to-peak interval, standard deviation, crest factor, mean square root, skewness, kurtosis, principal component analysis, time synchronous average, autoregressive model and autoregressive moving average (ARMA) model [3]. The simplest frequency domain analysis is spectral analysis by fast Fourier transform (FFT). Improvements in FFT processing have produced other techniques, such as envelope analysis, Hilbert transform, cepstrum analysis, bispectrum analysis, full spectrum, and also frequency-based parametric models, such as ARMA spectrum [4]. Time-frequency domain analyses are used in non-stationary signals where FFT does not produce accurate results (for example, in situations where rotational speed is not constant). For example, time-frequency techniques include short-time Fourier transform, Wavelet Transform or spectrogram (the power of STFT), Wigner–Ville distribution, Choi–Williams distribution, and order tracking techniques.

Machine diagnosis is done by pattern recognition in the processed signals. Research using AI approach for machine diagnostics has been on the increase over the last years. The most common AI approaches are fuzzy logic and [5, 6], neural networks [7, 8] and support vector machine [9].

A special form of treatment of FFT signals is analyzed for signal processing in current experiment. FFT is applied in complex signal or vibration. The complex

signal is formed by two real signals, perpendicular to each other. In this case, the full spectrum (negative and positive frequencies) of a complex signal gives more information about the dynamical behavior of the machine than the half spectrum of a real signal. There are several researches applying full spectrum technique for the two machine diagnoses [10-17] and for complex modal analysis [18-20]. However, the use of full spectrum technique coupled to an AI approach still demands research. In this context, current paper presents the development of a system for the diagnosis of rotating machines through fuzzy logic and employing rules based on full spectra of complex vibration signals of a rotor test rig. Full spectra plots were obtained by spectral density functions of the complex signals, i.e., by directional power spectral density function (dPSD) [18, 19]. The experiments were performed in a rotor test rig in which some types of mechanical faults were introduced: unbalancing, parallel and angular misalignment. Certain rules were established according to full spectra of the signals, corresponding to different fault types. Further, the diagnostic system based on Fuzzy Logic was developed using Matlab toolbox.

2. Complex Notation for Rotor Vibration Signal

Figure 1 shows a simple Jeffcott rotor in which the coordinates of the flexural motion (or whirl movement) are given by coordinates y and z. The complex coordinate is defined by

$$p(t) = y(t) + jz(t) \tag{1}$$

Therefore, in the complex plane, the y-axis becomes the real axis and the z-axis becomes the imaginary one, as indicated. The complex variable $p(t)$ may be also considered as the sum of two contra-rotating vectors, resulting in the shape of the rotor´s orbit [11, 13].

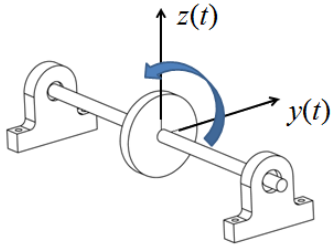

Fig. 1. Coordinates *y* and *z* describing the rotor´s flexural movement.

The Fourier transform of $p(t)$ is a complex quantity, but it is not an even function (as in traditional signal analysis) because $p(t)$ is not a real function. In other words, in the full spectrum of the magnitude of the Fourier transform of $p(t)$, the negative frequencies spectrum is not the mirror of the positive ones. In negative (positive) frequencies, information exists on the backward (forward) components. The identification of backward and forward components in rotors may lead to a more precise investigation of what kind of defect occurs in the machine. Goldman and Muszynska [13] presented a summary that showed some rotating machinery malfunctions and their respective full spectrum pattern.

Instead of using the magnitude of the Fourier Transform of $p(t)$ for full spectra plots, the power spectral density of $p(t)$, i. e. $S_{pp}(\omega)$, called the directional power spectral density function dPSD, may be used. The directional spectral density functions of a complex valued signal $p(t)$ may be defined in terms of the conventional auto- and cross-spectral density functions between $y(t)$ and $z(t)$ signals, as shown in references [18, 19]:

$$S_{pp}(\omega) = S_{yy}(\omega) + S_{zz}(\omega) + j\left(S_{yz}(\omega) - S_{zy}(\omega)\right) \tag{2}$$

$$S_{\overline{pp}}(\omega) = S_{yy}(\omega) - S_{zz}(\omega) + j\left(S_{yz}(\omega) + S_{zy}(\omega)\right) \tag{3}$$

where the quantity $S_{\overline{pp}}(\omega)$ is called the directional cross-spectral density function (dCSD). For real signals, the spectral density function complies with such symmetric properties as

$$S_{yy}(-\omega) = \overline{S}_{yy}(\omega) = S_{yy}(\omega),\ S_{yz}(-\omega) = \overline{S}_{yz}(\omega) = S_{zy}(\omega) \tag{4}$$

which implies that the conventional PSD, $S_{yy}(\omega)$, is a real, even function of ω, whereas the conventional CSD, $S_{yz}(\omega)$, is a complex-valued, conjugate even function of ω. The symbol ($\overline{\ }$) above some functions denotes the complex conjugate. Thus, the directional spectra satisfy

$$S_{pp}(-\omega) = S_{\overline{pp}}(\omega),\ S_{\overline{pp}}(\omega) = \overline{S}_{\overline{pp}}(\omega) = S_{\overline{pp}}(-\omega) \tag{5}$$

which suggests that the dPSD, $S_{pp}(\omega)$, of a complex signal is a real, but not necessarily even function of ω and the dCSD is a conjugate even function of ω.

The employment of full spectrum with intelligence computational techniques is not usual. Current assay uses full spectrum to analyze the distribution pattern of backward and forward components for each fault to define the rules necessary for the development of the fault diagnosis fuzzy system.

3. Experimental Results

In order to apply the proposed methodology, a rotor test rig was employed in which defects were inserted and the vibration signals in the radial directions were measured. Three different types of defects were inserted: unbalance, angular misalignment and parallel misalignment. When the radial vibration signals for each type of defect were measured, the complex signal for each situation was generated and its respective directional power spectral density function (DPSD) was obtained.

3.1. Experimental setup

Figure 2(a) shows the rotor test rig used to emulate the faulty behavior of a rotating machine. The test rig is MFS-RDS model from Spectra Quest Inc., comprising an electric motor drive, two ball bearings, one shaft with ½ inch diameter and 47 cm long, a claw coupling, and a disc (rotor) with holes for the insertion of the unbalanced mass. The two orthogonal accelerometers were fixed at the bearing closer to the electric motor.

The instruments comprised Wilcoxon accelerometers with data acquisition system, from National Instruments, controlled by a code in Labview software. After the measuring of the signals, they were processed in a Matlab code. The basic characteristics of the experimental setup for the vibration signals acquisition comprise: rotational speed of the machine: 23 Hz; time record: 4 s; window: hanning; and sampling frequency: 1 kHz.

In order to simulate the unbalance mass, a screw was inserted in the disc (see Fig. 2(b). Other defects inserted were the parallel and angular misalignments. The mechanism in the rotor test rig was used for the insertion of the misalignments, permitting such faults inserts. For more accurate analysis, several measurements were performed for unbalance and misalignment at different levels of severity.

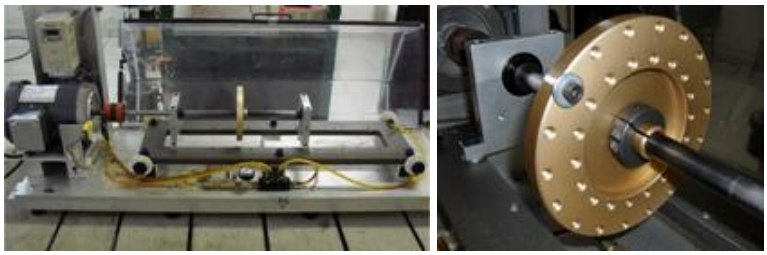

Fig. 2. (a) Rotor test rig, (b) Rotating disc with unbalance mass.

3.2. Vibration response of unbalanced rotor

Results revealed that the higher the unbalance level, the higher was the level of dPSD amplitude for both forward and backward components. The appearance of backward component suggests a level of anisotropy in the system. If the system were isotropic only, a forward component would appear (if only unbalance were present). Figure 3 corresponds to full spectrum of unbalance response when a mass of 13.79 g was placed in the rotor. All unbalanced masses were placed at a radial distance of 6 cm from the rotor´s center.

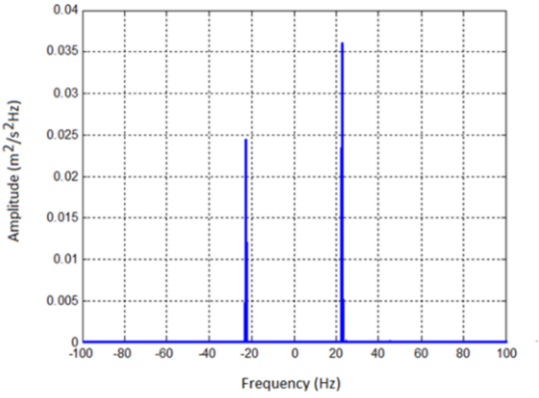

Fig. 3. Full spectrum corresponding to 13.74 g unbalanced mass.

3.3. Vibration response of rotor with angular misalignment

Figures 4(a)-(c) present dPSD plots for the system with different levels of angular misalignments. It is important to emphasize that misalignment is a non-linear and complex phenomenon. It is a function of combining type (stiffness), rotational speed and level of severity [21]. Thus, one or more peaks would appear in a traditional half spectrum corresponding to misalignment. Figure 4(a) shows that in the case of a low angular misalignment level, a result similar to an unbalance case occurs, i.e., there are components in 1*X* and -1*X* (*X* denotes the rotation of machine). When this misalignment level is higher, the peaks increase at the same proportion. There are also peaks in 3*X* and -3*X*, Fig. 4(b). In the case of the highest angular misalignment level, Fig. 4(c), the peak in 3*X* (-3*X*) becomes higher than peaks in 1*X* (-1*X*). In all situations, the system whirls in a forward direction (the peaks in the positive frequency are higher than the corresponding ones in negative frequency) [13].

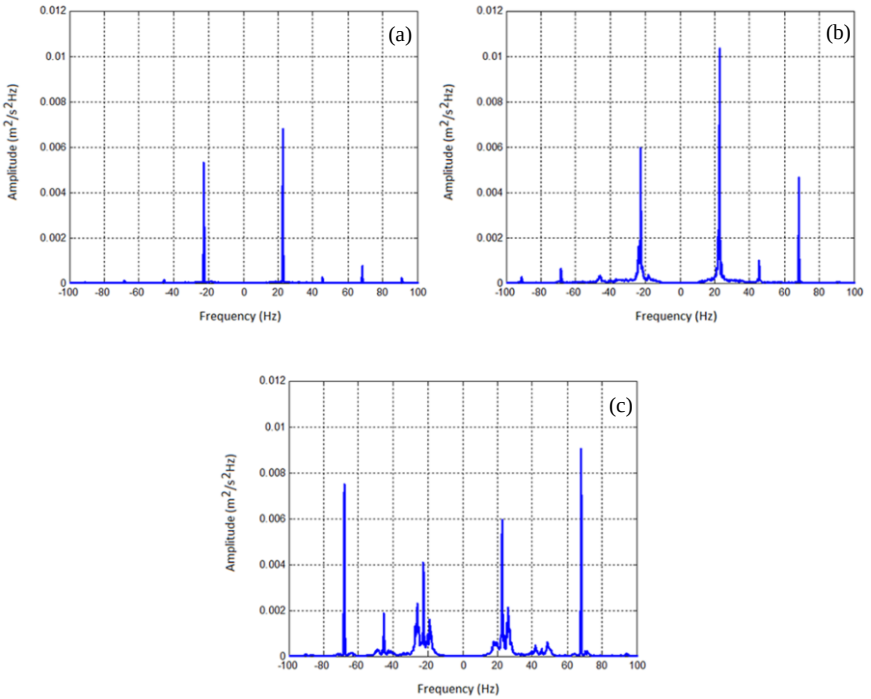

Fig. 4. Full spectra corresponding to angular misalignment: (a) α1=0.09º, (b) α2 = 0.135º, (c) α3 = 0.19º.

3.4. Vibration response of rotor with parallel misalignment

Figures 5(a)-(c) present dPSD plots for the system with different levels of parallel misalignments. When the misalignment is low, Fig. 5(a), the full spectrum will be similar to full spectrum for angular misalignment. Therefore, in the case of low misalignments, it is difficult to identify whether it is parallel or angular. When the parallel misalignment level increases, Fig. 5(b), the peaks in -3*X* and 3*X* will

become significant. When the severity is higher, Fig. 5(c), the peaks in 1*X* and 3*X* will become higher still when compared with the peaks in -1*X* and -3*X*, respectively. Differently from angular misalignment, the higher the level of parallel misalignment, the higher the positive components are in comparison with the corresponding negative ones. In the latter case, the appearance of other small peaks may be noted, probably due to nonlinearities triggered by high excitation levels.

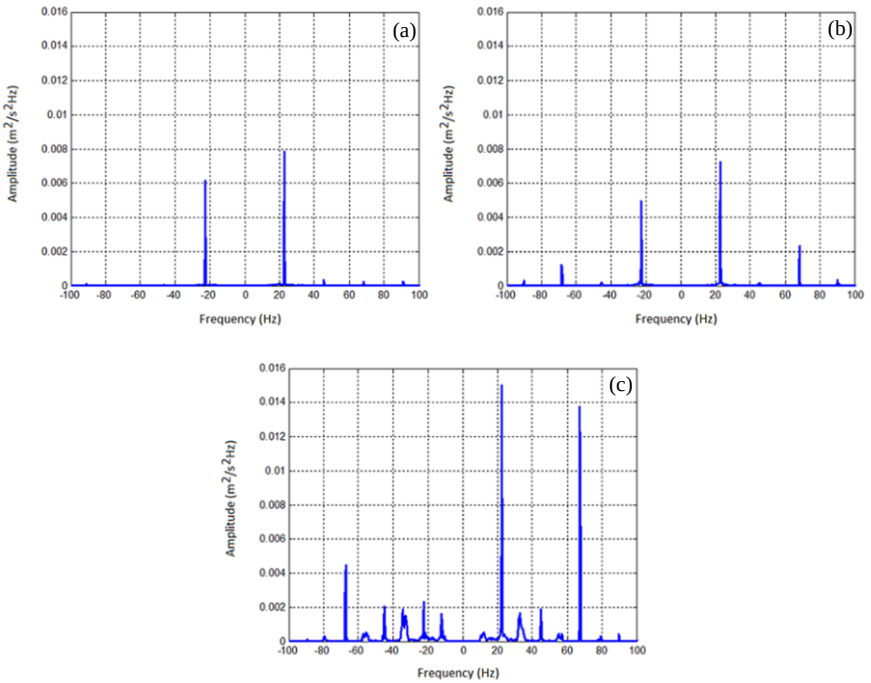

Fig. 5. Full spectra corresponding to parallel misalignment: (a) dy1= 0.7 mm, (b) dy2=1 mm, (c) dy3= 1.4 mm.

4. Fuzzy Diagnosis System

The proposed fuzzy diagnostic system has as objective to identify which fault is present in machine. The system uses as input the vibration overall RMS value and amplitudes from dPSD; and as output it produces the condition of the machine and the type of fault the machine presents.

4.1. Fuzzy Logic from overall RMS value of vibration and dPSD plots

According to results (dPSD plots and overall vibration level measured), a set of rules was developed to evaluate the severity of the vibration level and to identify which defect was present in the machine. Vibration severity was classified following recommendations of ISO 2372 for rotating machinery vibrations [22]. ISO 2372 criteria use the overall RMS value of vibration in velocity (mm/s), and the severity of defects in rotating machinery may be classified as Good (G),

Satisfactory (S), Unsatisfactory (Unsat) and Unacceptable (Unaccep). Fault type is identified by means of the pattern of occurrence of the first four, positive and negative, harmonics of dPSD full spectra, because they are sufficient to identify the unbalance and misalignment faults.

In current assay, the classification of RMS faults´ severity comprises "Low", "Medium" and "High". These linguistics values form the fuzzy sets and their respective membership functions for the input RMS, Fig. 6(a). The other fuzzy system inputs are the ratio of amplitudes between the amplitude of the first positive (negative) harmonic and the sum of the amplitudes of the first four positive (negative) harmonics. The same is performed for 2nd, 3rd and 4th harmonics. However, based on full spectrum analysis to identify the defects in the rotor test rig used, only the percentage ratio of the amplitudes of the third harmonic positive and negative ($A3X_+$ and $A3X_-$) are necessary, coupled to the sum of the first four amplitudes of the positive (or negative) harmonics, called $Y3_+$ (or $Y3_-$), respectively, i.e.

$$Y3_+ = \frac{A3X_+}{A1X_+ + A2X_+ + A3X_+ + A4X_+}100\% \quad (6)$$

$$Y3_- = \frac{A3X_-}{A1X_- + A2X_- + A3X_- + A4X_-}100\% \quad (7)$$

The ratios above are different for each fault and, consequently, they may be used to identify faults in the machine. Figure 6(b) shows the sets and membership functions for the two entries ($Y3_+$ and $Y3_-$). For the definition of the fuzzy sets, an analysis of several measurements was made considering all faults and their severities. It was decided to use 5 functions, Fig. 6(b) in order to avoid great number of rules, and their limits were defined according to the values of the measurements obtained from the rotor test rig.

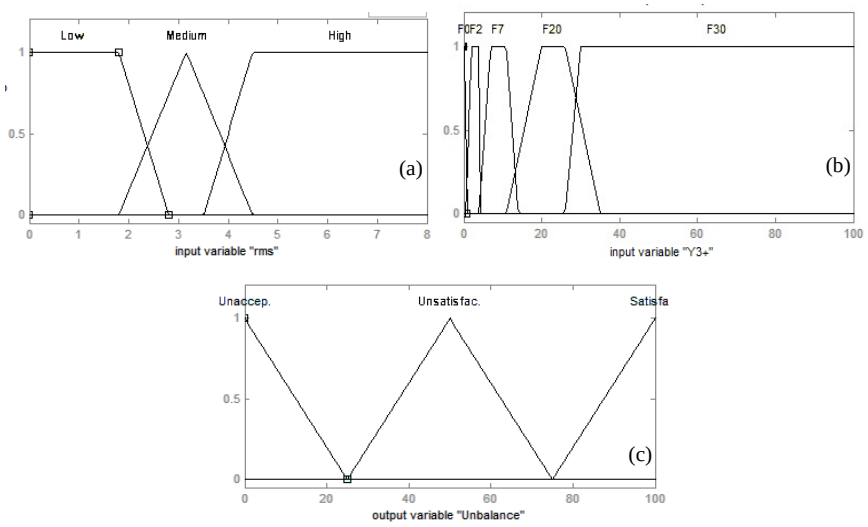

Fig. 6. (a) Fuzzy sets for overall RMS level, (b) Fuzzy sets for $Y3_+$ and $Y3_-$, (c) Fuzzy sets for outputs.

The fuzzy system outputs may be of two types: the condition of the machine and the type of defect it presents. In linguistic terms, these outputs are classified as Satisfactory, Unsatisfactory and Unacceptable, as shown respectively in Fig. 6(c). The fuzzy set in Fig. 6(c) is applied for the machine´s condition and for all types of defects.

4.2. Fuzzy Rules

A group of 14 rules were implemented from the results of the RMS vibration global value, and amplitude ratios from full spectra as explained previously. The rules were produced to indicate whether the machine was in good condition or whether a fault existed. In case of a fault, the rules identified the kind of failure and its severity. The set of rules is shown in Table 1.

Table 1. Fuzzy rules.

	Rule Description
01	If (RMS is B) then OperCond is Satisfactory
02	If (RMS is M) then OperCond is Unsatisfactory
03	If (RMS is A) then OperCond is Unacceptable
04	If (RMS is B) then Unbalance is Satisfactory
05	If (RMS is M) and ($Y3_+$ is F0) and ($Y3_-$ is F0) then Unbalance is Unsatisfactory
06	If (RMS is B) then Parallel_Misalignment is Satisfactory
07	If (RMS is M) and ($Y3_+$ is F20) and ($Y3_-$ is F7) then Parallel_Misalignment is Unsatisfactory
08	If (RMS is M) and ($Y3_+$ is F7) and ($Y3_-$ is F7) then Parallel_Misalignment is Unsatisfactory
09	If (RMS is A) and ($Y3_+$ is F7) and ($Y3_-$ is F7) then Parallel_Misalignment is Unacceptable
10	If (RMS is A) and ($Y3_+$ is F30) and ($Y3_-$ is F7) then Parallel_Misalignment is Unacceptable
11	If (RMS is B) then Angular_Misalignment is Satisfactory
12	If (RMS is M) and ($Y3_+$ is F7) and ($Y3_-$ is F2) then Angular_Misalignment is Unsatisfactory
13	If (RMS is A) and ($Y3_+$ is F20) and ($Y3_-$ is F2) then Angular_Misalignment is Unacceptable
14	If (RMS is A) and ($Y3_+$ is F30) and ($Y3_-$ is F30) then Angular_Misalignment is Unacceptable

In the fuzzy logic system, the Mamdani's fuzzy inference method, the Center Area defuzzificator, the "minimum" implication method, and "maximum" aggregation method were employed. The proposed fuzzy logic configuration was implemented in the Matlab fuzzy logic toolbox and then validated with the results of measurements from the rotor test rig for different faults.

4.3. Fuzzy Logic Results

According to the diagnostics provided by the fuzzy system, Tables 2 to 5 show the results of machine in good conditions and the results for faults introduced in the rotor test rig in various scenarios. For each fault, there are different degrees of severity. The results are the possibility (in percentage) of fault occurrence.

Table 2 presents the results for fault-less machine. The RMS value was around 2.4 mm/s. Value was considerable low, although residuals faults were still present. The diagnosis system shows a Good Machine Condition possibility of 62.9%, i.e., the machine has a vibration that does not imply any problems. The possibilities of unbalanced, parallel and angular misalignment were analyzed and showed satisfactory levels around 9.75%, i. e., all these defects have low occurrence possibility for this case.

Table 2. Results for machine in good conditions.

Fault Type:	Inputs			Machine Condition	Unbalance	Parallel Misalignment	Angular Misalignment
	RMS	Y3₋	Y3₊				
Machine without faults	2.4	3.9	3	62.9% (S)	9.75% (S)	9.75% (S)	9.75% (S)

In the case of the unbalanced machine (Table 3), when the unbalanced mass increases, the possibility of unbalance also increases. The possibility is 37.1% of unbalance for a 7.34g of unbalanced mass and reaches 92% unbalance for high 20.61g of unbalanced mass. However, other defects always have low values, confirming absence. In Table 4, for angular misalignment levels of 0.09º, 0.135º and 0.19º angular misalignments, the possibilities are 36.8%, 91.2% and 92%, respectively, while unbalance and parallel misalignment have low possibilities. Finally, for parallel misalignment levels of 0.7, 1.0 and 1.4 mm misalignments, the possibilities of parallel misalignment are 46.2%, 50% and 92%, respectively. Other defects show low occurrence possibility values. Therefore, the system identifies correctly all rotating machine defects and discards the occurrence of other defects.

Table 3. Results for unbalanced machine.

Fault Type: Unbalance	Inputs RMS	Y3₋	Y3₊	Machine Condition	Unbalance	Parallel Misalignment	Angular Misalignment
7.34g	2.4	0.5	0.4	62.9% (S)	37.1% (Unsat)	9.5% (S)	9.95% (S)
10.55g	3.2	0.2	0.1	50% (Unsat)	50% (Unsat)	0% (S)	0% (S)
13.79g	4.1	0	0	31.1% (Unaccep)	68.9% (Unaccep)	0% (S)	0% (S)
17.19g	4.8	0	0	8% (Unaccep)	92% (Unaccep)	0% (S)	0% (S)
20.61g	5.7	0	0	8% (Unaccep)	92% (Unaccep)	0% (S)	0% (S)

Table 4. Results for machine with angular misalignment.

Fault Type: Angular Misalign.	Inputs RMS	Y3₋	Y3₊	Machine Conditions	Unbalance	Parallel Misalignment	Angular Misalignment
0.09º	2.6	5.5	1	57% (Unsat)	11% (S)	11% (S)	36.8% (Unsat)
0.135º	5.4	17	2.2	8% (Unaccep)	0% (S)	0% (S)	91.2% (Unaccep)
0.19º	7.4	46	38	8% (Unaccep)	0% (S)	0% (S)	92% (Unaccep)

Table 5. Results for machine with parallel misalignment.

Fault Type: Parallel Misalign.	Inputs RMS	Y3₋	Y3₊	Machine Conditions	Unbalance	Parallel Misalignment	Angular Misalignment
0.7 mm	2.7	1.8	0.2	53.8% (Unsat)	11.6% (S)	46.2% (Unsat)	11.6% (S)
1.0 mm	3.4	14	7	50% (Unsat)	0% (S)	50% (Unsat)	0% (S)
1.4 mm	6.4	33	11	8% (Unaccep)	0% (S)	92% (Unaccep)	0% (S)

The methodology presented in the paper is classified as knowledge-based method, or pattern recognition approach [1, 23, 24], in contrast to model-based methods, where a mathematical representation of the physical behaviour of the system is required [1, 2, 23-25]. Therefore, to include additional faults in the proposed diagnostic system, more knowledge, more data are required, thus more rules will be necessary, and obviously more knowledge of the physics of the system is also necessary. For example, forces generated by unbalance and misalignment are forces that excite forward precession (the peaks in the positive frequency are higher than negatives ones), whereas forces generated by faults such as cracked rotor or rubbing, higher components of negative frequencies can be present in full spectra [13-15].

5. Conclusions

Fault diagnosis of rotating machines is essential for maintenance and cost savings. Since fault diagnosis based on artificial intelligence has increasingly been used, current paper presented a methodology that combined signal processing based on the full spectrum with the diagnosis by fuzzy logic so that diagnosis could be more effective.

Information from full spectra, i.e., spectra with positive and negative frequency from complex signals, forward more information on the system´s dynamics than the spectra of real signals of vibration (half spectra), and thus defects may be better distinguished. The diagnostic system was applied to a rotor test rig in which three different types of defects were inserted, one at a time, and the system was able to distinguish them successfully.

The diagnostic system may be expanded to support more defects, but new rules should be formulated with knowledge of the physics of the phenomenon. This is the first study by the authors to combine artificial intelligence techniques and full spectrum information to produce a more robust system so that it may be replicated on other machines and when neurofuzzy techniques are being analyzed.

References

1. Jardine, A.; Lin, D.; and Banjevic, D. (2006). A review on machinery diagnostics and prognostics implementing condition-based maintenance. *Mechanical Systems and Signal Processing*, 20, 1483-1510.
2. Friswell, M.; and He, Y. (2009). Smart rotating machines for condition monitoring. *Key Engineering Materials*, 413-414: 423-430.
3. Aherwar, A. (2012). An investigation on gearbox fault detection using vibration analysis techniques - A review. *Australian Journal of Mechanical Engineering*, 10(2), 169-184.
4. El-Thalji, I.; and Jantunen, E. (2015). Summary of fault modelling and predictive health monitoring of rolling element bearings. *Mechanical Systems and Signal Processing*, 60, 252-272.
5. Wang, H.; and Chen, P. (2011). Fuzzy diagnosis method for rotating machinery in variable rotating speed. *IEEE Sensors Journal*, 11(1), 23-34.

6. Aydin, I.; Karakose, M.; and Akin, E. (2014). An approach for automated fault diagnosis based on a fuzzy decision tree and boundary analysis of a reconstructed phase space. *ISA Transactions*, 53(2), 220-229.
7. Hussain, M.A.; Che Hassan, C.R.; Loh, K.S.; Mah, K.H. (2007). Application of artificial intelligence techniques in process fault diagnosis. *Journal of Engineering Science and Technology* (*JESTEC*), 2(3), 260-270.
8. Jia, F.; Lei, Y.; Lin, J.; Zhou, X.; and Lu, N. (2016). Deep neural networks: a promising tool for fault characteristic mining and intelligent diagnosis of rotating machinery with massive data. *Mechanical Systems and Signal Processing*, 72-73, 303-315.
9. Sakthivel, N.R.; Saravanamurugan, S.; Nair, B.B.; Elangova, M.; and Sugumaran, V. (2016). Effect of kernel function in support vector machine for the fault diagnosis of pump. *Journal of Engineering Science and Technology* (*JESTEC*), 11(6), 826-838.
10. Muszynska, A. (1996). Forward and backward precession of a vertical anisotropically supported rotor. *Journal of Sound and Vibration*, 192, 207-222.
11. Lee, C.W.; Vun-Sik Han, V.S.; and Park. J.P. (1997). Use of directional spectra for detection of engine cylinder power fault. *Shock and Vibration*, 4(5,6), 391-401.
12. Park, J.P.; and Lee, C.W. (1999). Diagnosis of faults in rolling element bearings by using directional spectra of vibration signals. *KSME International Journal*, 13(1), 63-73.
13. Goldman, P.; and Muszynska, A. (1999). Application of full spectrum to rotating machinery diagnostics. *Bently Nevada Orbit*, 20(1), 17-21.
14. Bently, D. (2002). *Fundamentals of rotating machinery diagnostics*. ASME Press, American Society of Mechanical Engineers.
15. Patel, T.H.; and Darpe, A.K. (2008). Vibration response of a cracked rotor in presence of rotor–stator rub. *Journal of Sound and Vibration*, 317, 841-865.
16. Patel, T.H.; and Darpe, A.K. (2009). Experimental investigations on vibration response of misaligned rotors. *Mechanical Systems and Signal Processing*, 23 (7), 2236-2252.
17. Southwick, D. (2011). Using Full Spectrum Plots. *Bently Nev. Orbit*, 14(4), 19-21.
18. Lee, C.W.; and Joh, C.Y. (1993). Theory of excitation methods and estimation of frequency response functions in complex modal testing of rotating machinery. *Mechanical systems and signal processing*, 7(1), 57-74.
19. Lee, C.W. (1997). An efficient Complex modal testing theory for asymmetric rotor systems: use of unidirectional excitation method. *Journal of Sound and Vibration*, 206 (3), 327-338.
20. Chouksey, M.; Dutt, J.K.; and Modak, S.V. (2012). Modal analysis of rotor-shaft system under the influence of rotor-shaft material damping and fluid film forces. *Mechanism and Machine Theory*, 48, 81-93.
21. Ganeriwala, S.; Patel, S.; and Hartunga, A. (1999). The truth behind misalignment vibration spectra of rotating machinery. In: *Proceedings of International Modal Analysis Conference*, Florida, USA, 2078-2205.
22. ISO 2372. (1974). *Mechanical vibration of machines with operating speeds from 10 to 200 rev/s - Basis for specifying evaluation standards*. International Standards Organizations, Geneva, Switzerland.

23. Tung, T.V.; and Yang, B. (2009). Machine fault diagnosis and prognosis: the state of the art. *International Journal of Fluid Machinery and Systems*, 2(1), 61-71.
24. Sikorska, J.Z.; Hodkiewicz, M.; and Ma, L. (2011). Prognostic modelling options for remaining useful life estimation by industry. *Mechanical Systems and Signal Processing*, 25, 1803-1836.
25. Less, A.W.; Sinha, J.K.; and Friswell, M.I. (2009). Model-based identification of rotating machines. *Mechanical Systems and Signal Processing*, 23, 1884-1893.